

Chapter 4

Local stability


It does not say in the Bible that all laws of nature are expressible linearly.

— Enrico Fermi

(R. Mainieri and P. Cvitanović)

SO FAR we have concentrated on describing the trajectory of a single initial point. Our next task is to define and determine the size of a *neighborhood* of $x(t)$. We shall do this by assuming that the flow is locally smooth and by describing the local geometry of the neighborhood by studying the flow linearized around $x(t)$. Nearby points aligned along the stable (contracting) directions remain in the neighborhood of the trajectory $x(t) = f^t(x_0)$; the ones to keep an eye on are the points which leave the neighborhood along the unstable directions. As we shall demonstrate in chapter 18, the expanding directions matter in hyperbolic systems. The repercussions are far-reaching. As long as the number of unstable directions is finite, the same theory applies to finite-dimensional ODEs, state space volume preserving Hamiltonian flows, and dissipative, volume contracting infinite-dimensional PDEs.

In order to streamline the exposition, in this chapter all examples are collected in sect. 4.8. We strongly recommend that you work through these examples: you can get to them and back to the text by clicking on the [example] links, such as

 [example 4.8](#)
[p. 87](#)

4.1 Flows transport neighborhoods

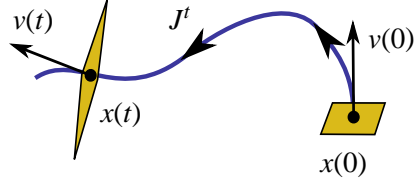
As a swarm of representative points moves along, it carries along and distorts neighborhoods. The deformation of an infinitesimal neighborhood is best understood by considering a trajectory originating near $x_0 = x(0)$, with an initial infinitesimal displacement $\delta x(0)$. The flow then transports the displacement $\delta x(t)$ along the trajectory $x(x_0, t) = f^t(x_0)$.



4.1.1 Instantaneous rate of shear

The system of linear *equations of variations* for the displacement of the infinitesimally close neighbor $x + \delta x$ follows from the flow equations (2.7) by Taylor

Figure 4.1: For finite times a local frame is transported along the orbit and deformed by Jacobian matrix J^t . As J^t is not self-adjoint, an initial orthogonal frame is mapped into a non-orthogonal one.



expanding to linear order

$$\dot{x}_i + \delta \dot{x}_i = v_i(x + \delta x) \approx v_i(x) + \sum_j \frac{\partial v_i}{\partial x_j} \delta x_j.$$

The infinitesimal displacement δx is thus transported along the trajectory $x(x_0, t)$, with time variation given by

$$\frac{d}{dt} \delta x_i(x_0, t) = \sum_j \left. \frac{\partial v_i}{\partial x_j}(x) \right|_{x=x(x_0, t)} \delta x_j(x_0, t). \tag{4.1}$$

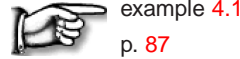
As both the displacement and the trajectory depend on the initial point x_0 and the time t , we shall often abbreviate the notation to $x(x_0, t) \rightarrow x(t) \rightarrow x$, $\delta x_i(x_0, t) \rightarrow \delta x_i(t) \rightarrow \delta x$ in what follows. Taken together, the set of equations

$$\dot{x}_i = v_i(x), \quad \delta \dot{x}_i = \sum_j A_{ij}(x) \delta x_j \tag{4.2}$$

governs the dynamics in the tangent bundle $(x, \delta x) \in \mathbf{TM}$ obtained by adjoining the d -dimensional tangent space $\delta x \in TM_x$ to every point $x \in M$ in the d -dimensional state space $M \subset \mathbb{R}^d$. The *stability matrix* or *velocity gradients matrix*

$$A_{ij}(x) = \frac{\partial v_i(x)}{\partial x_j} \tag{4.3}$$

describes the instantaneous rate of shearing of the infinitesimal neighborhood of $x(t)$ by the flow. A swarm of neighboring points of $x(t)$ is instantaneously sheared by the action of the stability matrix, $\delta x(t + \delta t) = \delta x(t) + \delta t A(x_t) \delta x(t)$. A is a tensorial rate of deformation, so it is a bit hard (if not impossible) to draw.



4.1.2 Finite time linearized flow

By Taylor expanding a *finite time* flow to linear order,

$$f_i^t(x_0 + \delta x) = f_i^t(x_0) + \sum_j \frac{\partial f_i^t(x_0)}{\partial x_{0j}} \delta x_j + \dots, \tag{4.4}$$

one finds that the linearized neighborhood is transported by the Jacobian matrix

$$\delta x(t) = J^t(x_0) \delta x_0, \quad J_{ij}^t(x_0) = \frac{\partial x(t)_i}{\partial x(0)_j}, \quad J^0(x_0) = \mathbf{1}. \tag{4.5}$$

remark 4.1

For example, in 2 dimensions the Jacobian matrix for change from initial to final coordinates is

$$J^t = \frac{\partial(x, y)}{\partial(x_0, y_0)} = \begin{pmatrix} \frac{\partial x}{\partial x_0} & \frac{\partial x}{\partial y_0} \\ \frac{\partial y}{\partial x_0} & \frac{\partial y}{\partial y_0} \end{pmatrix}.$$

The Jacobian matrix is evaluated on a trajectory segment that starts at point $x_0 = x(t_0)$ and ends at point $x_1 = x(t_1)$, $t_1 \geq t_0$. As the trajectory $x(t)$ is deterministic, the initial point x_0 and the elapsed time t in (4.5) suffice to determine J , but occasionally we find it helpful to be explicit about the initial and final times and state space positions, and write

$$J_{ij}^{t_1-t_0} = J_{ij}(t_1; t_0) = J_{ij}(x_1, t_1; x_0, t_0) = \frac{\partial x(t_1)_i}{\partial x(t_0)_j}. \quad (4.6)$$

The map f^t is assumed invertible and differentiable so that J^t exists. For sufficiently short times J^t remains close to $\mathbf{1}$, so $\det J^t > 0$. By continuity $\det J^t$ remains positive for all times t . However, for discrete time maps, $\det J^n$ can have either sign.

4.1.3 Co-moving frames

J describes the deformation of an infinitesimal neighborhood at a finite time t in the co-moving frame of $x(t)$. This deformation of an initial frame at x_0 into a non-orthogonal frame at $x(t)$ is described by the eigenvectors and eigenvalues of the Jacobian matrix of the linearized flow (see figure 4.1),

$$J^t \mathbf{e}^{(j)} = \Lambda_j \mathbf{e}^{(j)}, \quad j = 1, 2, \dots, d. \quad (4.7)$$

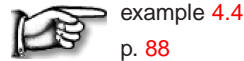
Throughout this text the symbol Λ_k will always denote the k th *eigenvalue* (the *stability multiplier*) of the finite time Jacobian matrix J^t . Symbol $\lambda^{(k)}$ will be reserved for the k th *stability exponent*, with real part $\mu^{(k)}$ and phase $\omega^{(k)}$:

$$\Lambda_k = e^{t\lambda^{(k)}} \quad \lambda^{(k)} = \mu^{(k)} + i\omega^{(k)}. \quad (4.8)$$

As J^t is a real matrix, its eigenvalues are either real or come in complex conjugate pairs,

$$\{\Lambda_k, \Lambda_{k+1}\} = \{e^{t(\mu^{(k)} + i\omega^{(k)})}, e^{t(\mu^{(k)} - i\omega^{(k)})}\},$$

with magnitude $|\Lambda_k| = |\Lambda_{k+1}| = \exp(t\mu^{(k)})$. The phase $\omega^{(k)}$ describes the rotation velocity in the plane spanned by the pair of real eigenvectors, $\{\text{Re } \mathbf{e}^{(k)}, \text{Im } \mathbf{e}^{(k)}\}$, with one period of rotation given by $T = 2\pi/\omega^{(k)}$.



example 4.4

p. 88

$J^t(x_0)$ depends on the initial point x_0 and the elapsed time t . For notational brevity we omitted this dependence, but in general both the eigenvalues and the eigenvectors, $\Lambda_j = \Lambda_j(x_0, t)$, \dots , $\mathbf{e}^{(j)} = \mathbf{e}^{(j)}(x_0, t)$, also depend on the trajectory traversed.

Nearby trajectories separate exponentially with time along the *unstable directions*, approach each other along the *stable directions*, and change their distance

along the *marginal directions* at rates slower than exponential, corresponding to the eigenvalues of the Jacobian matrix with magnitude larger than, smaller than, or equal to 1. In the literature, the adjectives *neutral*, *indifferent*, *center* are often used instead of ‘marginal’. Attracting, or stable directions are sometimes called ‘asymptotically stable,’ and so on.

One of the preferred directions is what one might expect, the direction of the flow itself. To see that, consider two initial points along a trajectory separated by infinitesimal flight time δt : $\delta x_0 = f^{\delta t}(x_0) - x_0 = v(x_0)\delta t$. By the semigroup property of the flow, $f^{t+\delta t} = f^{\delta t+t}$, where

$$f^{\delta t+t}(x_0) = \int_t^{\delta t+t} d\tau v(x(\tau)) + f^t(x_0) = \delta t v(x(t)) + f^t(x_0).$$

Expanding both sides of $f^t(f^{\delta t}(x_0)) = f^{\delta t}(f^t(x_0))$, keeping the leading term in δt , and using the definition of the Jacobian matrix (4.5), we observe that $J^t(x_0)$ transports the velocity vector at x_0 to the velocity vector at $x(t)$ (see figure 4.1):

$$v(x(t)) = J^t(x_0)v(x_0). \quad (4.9)$$

4.2 Computing the Jacobian matrix

As we started by assuming that we know the equations of motion, from (4.3) we also know stability matrix A , the instantaneous rate of shear of an infinitesimal neighborhood $\delta x_i(t)$ of the trajectory $x(t)$. What we do not know is the finite time deformation (4.5), so our next task is to relate the stability matrix A to Jacobian matrix J^t . On the level of differential equations the relation follows by taking the time derivative of (4.5) and replacing δx by (4.2)

$$\frac{d}{dt} \delta x(t) = \frac{dJ^t}{dt} \delta x_0 = A \delta x(t) = AJ^t \delta x_0.$$

Hence the matrix elements of the $[d \times d]$ Jacobian matrix satisfy the ‘tangent linear equations’

$$\frac{d}{dt} J^t(x_0) = A(x) J^t(x_0), \quad x = f^t(x_0), \quad \text{initial condition } J^0(x_0) = \mathbf{1}. \quad (4.10)$$

For autonomous flows, the matrix of velocity gradients $A(x)$ depends only on x , not time, while J^t depends on both the state space position and time. Given a numerical routine for integrating the equations of motion, evaluation of the Jacobian matrix requires minimal additional programming effort; one simply extends the d -dimensional integration routine and integrates the d^2 elements of $J^t(x_0)$ concurrently with $f^t(x_0)$. The qualifier ‘simply’ is perhaps too glib. Integration will work for short finite times, but for exponentially unstable flows one quickly runs into numerical over- and/or underflow problems. For high-dimensional flows the analytical expressions for elements of A might be so large that A fits on no computer. Further thought will have to go into implementation this calculation.

So now we know how to compute Jacobian matrix J^t given the stability matrix A , at least when the d^2 extra equations are not too expensive to compute. Mission accomplished.



fast track:

chapter 7, p. 134

And yet... there are mopping up operations left to do. We persist until we derive the integral formula (4.19) for the Jacobian matrix, an analogue of the finite-time ‘Green’s function’ or ‘path integral’ solutions of other linear problems.

We are interested in smooth, differentiable flows. If a flow is smooth, in a sufficiently small neighborhood it is essentially linear. Hence the next section, which might seem an embarrassment (what is a section on *linear* flows doing in a book on *nonlinear* dynamics?), offers a firm stepping stone on the way to understanding nonlinear flows. Linear charts are the key tool of differential geometry, general relativity, etc., so we are in good company. If you know your eigenvalues and eigenvectors, you may prefer to fast forward here.



fast track:

sect. 4.4, p. 81

4.3 A linear diversion

Linear is good, nonlinear is bad.

—Jean Bellissard

Linear fields are the simplest vector fields, described by linear differential equations which can be solved explicitly, with solutions that are good for all times. The state space for linear differential equations is $\mathcal{M} = \mathbb{R}^d$, and the equations of motion (2.7) are written in terms of a vector x and a constant stability matrix A as

$$\dot{x} = v(x) = Ax. \quad (4.11)$$

Solving this equation means finding the state space trajectory

$$x(t) = (x_1(t), x_2(t), \dots, x_d(t))$$

passing through a given initial point x_0 . If $x(t)$ is a solution with $x(0) = x_0$ and $y(t)$ another solution with $y(0) = y_0$, then the linear combination $ax(t) + by(t)$ with $a, b \in \mathbb{R}$ is also a solution, but now starting at the point $ax_0 + by_0$. At any instant in time, the space of solutions is a d -dimensional vector space, spanned by a basis of d linearly independent solutions.

How do we solve the linear differential equation (4.11)? If instead of a matrix equation we have a scalar one, $\dot{x} = \lambda x$, the solution is $x(t) = e^{t\lambda} x_0$. In order to solve the d -dimensional matrix case, it is helpful to rederive this solution by studying what happens for a short time step δt . If time $t = 0$ coincides with position $x(0)$, then

$$\frac{x(\delta t) - x(0)}{\delta t} = \lambda x(0), \quad (4.12)$$

which we iterate m times to obtain Euler’s formula for compounding interest

$$x(t) \approx \left(1 + \frac{t}{m}\lambda\right)^m x(0) \approx e^{t\lambda} x(0). \quad (4.13)$$

The term in parentheses acts on the initial condition $x(0)$ and evolves it to $x(t)$ by taking m small time steps $\delta t = t/m$. As $m \rightarrow \infty$, the term in parentheses converges to e^{tA} . Consider now the matrix version of equation (4.12):

$$\frac{x(\delta t) - x(0)}{\delta t} = Ax(0). \tag{4.14}$$

A representative point x is now a vector in \mathbb{R}^d acted on by the matrix A , as in (4.11). Denoting by $\mathbf{1}$ the identity matrix, and repeating the steps (4.12) and (4.13) we obtain Euler’s formula for the exponential of a matrix:

$$x(t) = J^t x(0), \quad J^t = e^{tA} = \lim_{m \rightarrow \infty} \left(\mathbf{1} + \frac{t}{m} A \right)^m. \tag{4.15}$$

We will find this definition for the exponential of a matrix helpful in the general case, where the matrix $A = A(x(t))$ varies along a trajectory.

Now that we have some feeling for the qualitative behavior of eigenvectors and eigenvalues of linear flows, we are ready to return to the nonlinear case. How do we compute the exponential (4.15)?



example 4.2
p. 87



fast track:
sect. 4.4, p. 81

section 5.2.1

Henriette Roux: So, computing eigenvalues and eigenvectors seems like a good thing. But how do you really do it?

A: Any text on numerics of matrices discusses how this is done; the keywords are ‘Gram-Schmidt’, and for high-dimensional flows ‘Krylov subspace’ and ‘Arnoldi iteration’. Conceptually (but not for numerical purposes) we like the economical description of neighborhoods of equilibria and periodic orbits afforded by projection operators. The requisite linear algebra is standard. As this is a bit of sidetrack that you will find confusing at the first go, it is relegated to appendix C.

4.4 Stability of flows



How do you determine the eigenvalues of the finite time local deformation J^t for a general nonlinear smooth flow? The Jacobian matrix is computed by integrating the equations of variations (4.2)

$$x(t) = f^t(x_0), \quad \delta x(x_0, t) = J^t(x_0) \delta x(x_0, 0). \tag{4.16}$$

The equations are linear, so we should be able to integrate them—but in order to make sense of the answer, we derive this integral step by step.

Consider the case of a general, non-stationary trajectory $x(t)$. The exponential of a constant matrix can be defined either by its Taylor series expansion or in terms of the Euler limit (4.15):

$$e^{tA} = \sum_{k=0}^{\infty} \frac{t^k}{k!} A^k = \lim_{m \rightarrow \infty} \left(\mathbf{1} + \frac{t}{m} A \right)^m. \tag{4.17}$$

Taylor expanding is fine if A is a constant matrix. However, only the second, tax-accountant’s discrete step definition of an exponential is appropriate for the task at hand. For dynamical systems, the local rate of neighborhood distortion

$A(x)$ depends on where we are along the trajectory. The linearized neighborhood is deformed along the flow, and the m discrete time-step approximation to J^t is therefore given by a generalization of the Euler product (4.17):

$$\begin{aligned} J^t(x_0) &= \lim_{m \rightarrow \infty} \prod_{n=m}^1 (\mathbf{1} + \delta t A(x_n)) = \lim_{m \rightarrow \infty} \prod_{n=m}^1 e^{\delta t A(x_n)} \\ &= \lim_{m \rightarrow \infty} e^{\delta t A(x_m)} e^{\delta t A(x_{m-1})} \dots e^{\delta t A(x_2)} e^{\delta t A(x_1)}, \end{aligned} \tag{4.18}$$

where $\delta t = (t - t_0)/m$, and $x_n = x(t_0 + n\delta t)$. Indexing of the product indicates that the successive infinitesimal deformation are applied by multiplying from the left. The $m \rightarrow \infty$ limit of this procedure is the formal integral

$$J_{ij}^t(x_0) = \left[\mathbf{T} e^{\int_0^t d\tau A(x(\tau))} \right]_{ij}, \tag{4.19}$$

where \mathbf{T} stands for time-ordered integration, *defined* as the continuum limit of successive multiplications (4.18). This integral formula for J^t is the main conceptual result of the present chapter. This formula is the finite time companion of the differential definition (4.10). The definition makes evident important properties of Jacobian matrices, such as their being multiplicative along the flow,

exercise 4.5

$$J^{t+t'}(x) = J^t(x') J^{t'}(x), \quad \text{where } x' = f^{t'}(x_0), \tag{4.20}$$

which is an immediate consequence of the time-ordered product structure of (4.18). However, in practice J is evaluated by integrating (4.10) along with the ODEs that define a particular flow.

4.5 Stability of maps



The transformation of an infinitesimal neighborhood of a trajectory under the iteration of a map follows from Taylor expanding the iterated mapping at finite time n to linear order, as in (4.4). The linearized neighborhood is transported by the Jacobian matrix evaluated at a discrete set of times $n = 1, 2, \dots$,

$$J_{ij}^n(x_0) = \left. \frac{\partial f_i^n(x)}{\partial x_j} \right|_{x=x_0}. \tag{4.21}$$

As in the finite time case (4.8), we denote by Λ_k the k th *eigenvalue* or multiplier of the finite time Jacobian matrix J^n . There is really no difference from the continuous time case, other than that now the Jacobian matrix is evaluated at integer times.



example 4.9
p. 91

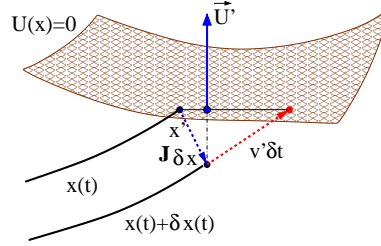
The formula for the linearization of n th iterate of a d -dimensional map

$$J^n(x_0) = J(x_{n-1}) \dots J(x_1) J(x_0), \quad x_j = f^j(x_0), \tag{4.22}$$

in terms of single time steps $J_{jl} = \partial f_j / \partial x_l$ follows from the chain rule for functional composition,

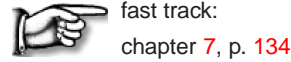
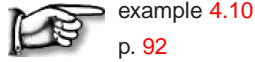
$$\frac{\partial}{\partial x_i} f_j(f(x)) = \sum_{k=1}^d \left. \frac{\partial f_j(y)}{\partial y_k} \right|_{y=f(x)} \frac{\partial f_k(x)}{\partial x_i}.$$

Figure 4.2: If $x(t)$ intersects the Poincaré section \mathcal{P} at time τ , the nearby $x(t) + \delta x(t)$ trajectory intersects it time $\tau + \delta t$ later. As $(U' \cdot v' \delta t) = -(U' \cdot J \delta x)$, the difference in arrival times is given by $\delta t = -(U' \cdot J \delta x)/(U' \cdot v')$.



If you prefer to think of a discrete time dynamics as a sequence of Poincaré section returns, then (4.22) follows from (4.20): Jacobian matrices are multiplicative along the flow.

exercise 6.3



4.6 Stability of Poincaré return maps

(R. Paškauskas and P. Cvitanović)



We now relate the linear stability of the Poincaré return map $P : \mathcal{P} \rightarrow \mathcal{P}$ defined in sect. 3.1 to the stability of the continuous time flow in the full state space.

The hypersurface \mathcal{P} can be specified implicitly through a function $U(x)$ that is zero whenever a point x is on the Poincaré section. A nearby point $x + \delta x$ is in the hypersurface \mathcal{P} if $U(x + \delta x) = 0$, and the same is true for variations around the first return point $x' = x(\tau)$, so expanding $U(x')$ to linear order in variation δx restricted to the Poincaré section, and applying the chain rule leads to the condition

$$\sum_{i=1}^d \frac{\partial U(x')}{\partial x_i} \frac{dx'_i}{dx_j} \Big|_{\mathcal{P}} = 0. \quad (4.23)$$

In what follows $U_i = \partial_j U$ is the gradient of U defined in (3.3), unprimed quantities refer to the starting point $x = x_0 \in \mathcal{P}$, $v = v(x_0)$, and the primed quantities to the first return: $x' = x(\tau)$, $v' = v(x')$, $U' = U(x')$. For brevity we shall also denote the full state space Jacobian matrix at the first return by $J = J^\tau(x_0)$. Both the first return x' and the time of flight to the next Poincaré section $\tau(x)$ depend on the starting point x , so the Jacobian matrix

$$\hat{J}(x)_{ij} = \frac{dx'_i}{dx_j} \Big|_{\mathcal{P}} \quad (4.24)$$

with both initial and the final variation constrained to the Poincaré section hypersurface \mathcal{P} is related to the continuous flow Jacobian matrix by

$$\frac{dx'_i}{dx_j} \Big|_{\mathcal{P}} = \frac{\partial x'_i}{\partial x_j} + \frac{dx'_i}{d\tau} \frac{d\tau}{dx_j} = J_{ij} + v'_i \frac{d\tau}{dx_j}.$$

The return time variation $d\tau/dx$, figure 4.2, is eliminated by substituting this expression into the constraint (4.23),

$$0 = \partial_i U' J_{ij} + (v' \cdot \partial U') \frac{d\tau}{dx_j},$$

yielding the projection of the full space d -dimensional Jacobian matrix to the Poincaré map $(d-1)$ -dimensional Jacobian matrix:

$$\hat{J}_{ij} = \left(\delta_{ik} - \frac{v'_i \partial_k U'}{(v' \cdot \partial U')} \right) J_{kj}. \quad (4.25)$$

Substituting (4.9) we verify that the initial velocity $v(x)$ is a zero-eigenvector of \hat{J}

$$\hat{J}v = 0, \quad (4.26)$$

so the Poincaré section eliminates variations parallel to v , and \hat{J} is a rank $(d-1)$ -dimensional matrix, i.e., one less than the dimension of the continuous time flow.

4.7 Neighborhood volume

Consider a small state space volume $\Delta V = d^d x$ centered around the point x_0 at time $t = 0$. The volume $\Delta V'$ around the point $x' = x(t)$ time t later is

$$\Delta V' = \frac{\Delta V'}{\Delta V} \Delta V = \left| \det \frac{\partial x'}{\partial x} \right| \Delta V = \left| \det J^t(x_0) \right| \Delta V, \quad (4.27)$$

so the $|\det J|$ is the ratio of the initial and the final volumes. The determinant $\det J^t(x_0) = \prod_{i=1}^d \Lambda_i(x_0, t)$ is the product of the Jacobian matrix eigenvalues. We shall refer to this determinant as the *Jacobian* of the flow. The Jacobian is easily evaluated. Take the time derivative, use the J evolution equation (4.10) and the matrix identity $\ln \det J = \text{tr} \ln J$:

$$\frac{d}{dt} \ln \Delta V(t) = \frac{d}{dt} \ln \det J = \text{tr} \frac{d}{dt} \ln J = \text{tr} \frac{1}{J} \dot{J} = \text{tr} A = \partial_i v_i.$$

(Here, as elsewhere in this book, a repeated index implies summation.) Integrate both sides to obtain the time evolution of an infinitesimal volume (Liouville's formula)

$$\det J^t(x_0) = \exp \left[\int_0^t d\tau \text{tr} \mathbf{A}(x(\tau)) \right] = \exp \left[\int_0^t d\tau \partial_i v_i(x(\tau)) \right]. \quad (4.28)$$

As the divergence $\partial_i v_i$ is a scalar quantity, the integral in the exponent (4.19) needs *no time ordering*. So all we need to do is evaluate the time average

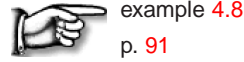
$$\begin{aligned} \overline{\partial_i v_i} &= \lim_{t \rightarrow \infty} \frac{1}{t} \int_0^t d\tau \sum_{i=1}^d A_{ii}(x(\tau)) \\ &= \frac{1}{t} \ln \left| \prod_{i=1}^d \Lambda_i(x_0, t) \right| = \sum_{i=1}^d \lambda^{(i)}(x_0, t) \end{aligned} \quad (4.29)$$

along the trajectory. If the flow is not singular (for example, the trajectory does not run head-on into the Coulomb $1/r$ singularity), the stability matrix elements are bounded everywhere, $|A_{ij}| < M$, and so is the trace $\sum_i A_{ii}$. The time integral in (4.29) thus grows at most linearly with t , $\partial_i v_i$ is bounded for all times, and numerical estimates of the $t \rightarrow \infty$ limit in (4.29) are not marred by any blowups. In numerical evaluations of stability exponents, the sum rule (4.29) can serve as a helpful check on the accuracy of the computation.



section 6.2
remark 6.1

exercise 4.1



example 4.8
p. 91

The divergence $\partial_i v_i$ characterizes the behavior of a state space volume in the infinitesimal neighborhood of the trajectory. If $\partial_i v_i < 0$, the flow is *locally contracting*, and the trajectory might be falling into an attractor. If $\partial_i v_i(x) < 0$, for all $x \in \mathcal{M}$, the flow is *globally contracting*, and the dimension of the attractor is necessarily smaller than the dimension of state space \mathcal{M} . If $\partial_i v_i = 0$, the flow preserves state space volume and $\det J^t = \mathbf{1}$. A flow with this property is called *incompressible*. An important class of such flows are the Hamiltonian flows considered in sect. 7.3.

But before we can get to that, Henriette Roux, the perfect student and always alert, pipes up. She does not like our definition of the Jacobian matrix in terms of the time-ordered exponential (4.19). Depending on the signs of multipliers, the left hand side of (4.28) can be either positive or negative. But the right hand side is an exponential of a real number, and that can only be positive. What gives? As we shall see much later on in this text, in discussion of topological indices arising in semiclassical quantization, this is not at all a dumb question.

Résumé

A neighborhood of a trajectory deforms as it is transported by a flow. In the linear approximation, the stability matrix A describes the shearing / compression / expansion of an infinitesimal neighborhood in an infinitesimal time step. The deformation after a finite time t is described by the Jacobian matrix

$$J^t(x_0) = \mathbf{T} e^{\int_0^t d\tau A(x(\tau))},$$

where \mathbf{T} stands for the time-ordered integration, defined multiplicatively along the trajectory. For discrete time maps this is multiplication by time-step Jacobian matrix J along the n points $x_0, x_1, x_2, \dots, x_{n-1}$ on the trajectory of x_0 ,

$$J^n(x_0) = J(x_{n-1})J(x_{n-2}) \cdots J(x_1)J(x_0),$$

where $J(x)$ is the single discrete time-step Jacobian matrix. In ChaosBook the *stability multiplier* Λ_k denotes the k th *eigenvalue* of the finite time Jacobian matrix $J^t(x_0)$, $\mu^{(k)}$ the real part of k th *stability exponent*, and $\omega^{(k)}$ its phase,

$$\Lambda = e^{t(\mu+i\omega)}.$$

For complex eigenvalue pairs the ‘angular velocity’ ω describes rotational motion in the plane spanned by the real and imaginary parts of the corresponding pair of complex eigenvectors.

The eigenvalues and eigen-directions of the Jacobian matrix describe the deformation of an initial infinitesimal cloud of neighboring trajectories into a distorted cloud at a finite time t later. Nearby trajectories separate exponentially along unstable eigen-directions, approach each other along stable directions, and change slowly (algebraically) their distance along marginal or center directions. The Jacobian matrix J^t is in general neither symmetric, nor diagonalizable by a rotation, nor do its (left or right) eigenvectors define an orthonormal coordinate

frame. Furthermore, although the Jacobian matrices are multiplicative along the flow, their eigenvalues are generally not multiplicative in dimensions higher than one. This lack of a multiplicative nature for eigenvalues has important repercussions for both classical and quantum dynamics.

Commentary

Remark 4.1 Linear flows. The subject of linear algebra generates innumerable tomes of its own; in sect. 4.3 we only sketch, and in appendix C recapitulate a few facts that our narrative relies on: a useful reference book is Meyer [1]. The basic facts are presented at length in many textbooks. Frequently cited linear algebra references are Golub and Van Loan [2], Coleman and Van Loan [3], and Watkins [4, 5]. The standard references that exhaustively enumerate and explain all possible cases are Hirsch and Smale [6] and Arnol'd [7]. A quick overview is given by Izhikevich [8]; for different notions of orbit stability see Holmes and Shea-Brown [9]. For ChaosBook purposes, we enjoyed the discussion in chapter 2 Meiss [10], chapter 1 of Perko [11] and chapters 3 and 5 of Glendinning [12]; we also liked the discussion of norms, least square problems, and differences between singular value and eigenvalue decompositions in Trefethen and Bau [13]. Truesdell [2] and Gurtin [3] are excellent references for the continuum mechanics perspective on state space dynamics; for a gentle introduction to parallels between dynamical systems and continuum mechanics see Christov *et al.* [1].

The nomenclature tends to be a bit confusing. A Jacobian matrix (4.5) is sometimes referred to as the *fundamental solution matrix* or simply *fundamental matrix*, a name inherited from the theory of linear ODEs, or the *Fréchet derivative* of the nonlinear mapping $f^t(x)$, or the ‘*tangent linear propagator*’, or even as the ‘*error matrix*’ (Lorenz [14]). The formula (4.22) for the linearization of n th iterate of a d -dimensional map is called a *linear cocycle*, a *multiplicative cocycle*, a *derivative cocycle* or simply a *cocycle* by some. Since matrix J describes the deformation of an infinitesimal neighborhood at a finite time t in the co-moving frame of $x(t)$, in continuum mechanics it is called a *deformation gradient* or a *transplacement gradient*. It is often denoted Df , but for our needs (we shall have to sort through a plethora of related Jacobian matrices) matrix notation J is more economical. Single discrete time-step Jacobian $J_{jt} = \partial f_j / \partial x_i$ in (4.22) is referred to as the ‘*tangent map*’ by Skokos [16, 17]. For a discussion of ‘*fundamental matrix*’ see appendix C.2.

We follow Tabor [15] in referring to A in (4.3) as the ‘*stability matrix*’; it is also referred to as the ‘*velocity gradients matrix*’ or ‘*velocity gradient tensor*’. It is the natural object for study of stability of equilibria, time-invariant point in state space; stability of trajectories is described by Jacobian matrices. Goldhirsch, Sulem, and Orszag [18] call it the ‘*Hessenberg matrix*’, and to the equations of variations (4.1) as ‘*stability equations*.’ Manos *et al.* [19] refer to (4.1) as the ‘*variational equations*’.

Sometimes A , which describes the instantaneous shear of the neighborhood of $x(x_0, t)$, is referred to as the ‘*Jacobian matrix*,’ a particularly unfortunate usage when one considers linearized stability of an equilibrium point (5.1). A is not a Jacobian matrix, just as a generator of SO(2) rotation is not a rotation; A is a generator of an infinitesimal time step deformation, $J^{\delta t} \simeq \mathbf{1} + A\delta t$. What Jacobi had in mind in his 1841 fundamental paper [20] on determinants (today known as ‘*Jacobians*’) were transformations between different coordinate frames. These are dimensionless quantities, while dimensionally A_{ij} is 1/[time].

More unfortunate still is referring to the Jacobian matrix $J^t = \exp(tA)$ as an ‘*evolution operator*,’ which here (see sect. 17.2) refers to something altogether different. In this book Jacobian matrix J^t always refers to (4.5), the linearized deformation after a finite time t , either for a continuous time flow, or a discrete time mapping.

4.8 Examples

10. Try to leave out the part that readers tend to skip.
— Elmore Leonard's Ten Rules of Writing.

The reader is urged to study the examples collected here. If you want to return back to the main text, click on [click to return] pointer on the margin.

Example 4.1 Rössler and Lorenz flows, linearized: (continued from example 3.5) For the Rössler (2.23) and Lorenz (2.18) flows, the stability matrices are respectively

$$A_{Ross} = \begin{pmatrix} 0 & -1 & -1 \\ 1 & a & 0 \\ z & 0 & x-c \end{pmatrix}, \quad A_{Lor} = \begin{pmatrix} -\sigma & \sigma & 0 \\ \rho-z & -1 & x \\ y & x & -b \end{pmatrix}. \quad (4.30)$$

(continued in example 4.5)

[click to return: p. 77](#)

Example 4.2 Jacobian matrix eigenvalues, diagonalizable case: Should we be so lucky that $A = A_D$ happens to be a diagonal matrix with eigenvalues $(\lambda^{(1)}, \lambda^{(2)}, \dots, \lambda^{(d)})$, the exponential is simply

$$J^t = e^{tA_D} = \begin{pmatrix} e^{t\lambda^{(1)}} & \dots & 0 \\ & \ddots & \\ 0 & \dots & e^{t\lambda^{(d)}} \end{pmatrix}. \quad (4.31)$$

Next, suppose that A is diagonalizable and that U is a nonsingular matrix that brings it to a diagonal form $A_D = U^{-1}AU$. Then J can also be brought to a diagonal form (insert factors $\mathbf{1} = UU^{-1}$ between the terms of the product (4.15)):

[exercise 4.2](#)

$$J^t = e^{tA} = Ue^{tA_D}U^{-1}. \quad (4.32)$$

The action of both A and J is very simple; the axes of orthogonal coordinate system where A is diagonal are also the eigen-directions of J^t , and under the flow the neighborhood is deformed by a multiplication by an eigenvalue factor for each coordinate axis.

We recapitulate the basic facts of linear algebra in appendix C. The following 2-dimensional example serves well to highlight the most important types of linear flows:

Example 4.3 Linear stability of 2-dimensional flows: For a 2-dimensional flow the eigenvalues $\lambda^{(1)}, \lambda^{(2)}$ of A are either real, leading to a linear motion along their eigenvectors, $x_j(t) = x_j(0) \exp(t\lambda^{(j)})$, or form a complex conjugate pair $\lambda^{(1)} = \mu + i\omega$, $\lambda^{(2)} = \mu - i\omega$, leading to a circular or spiral motion in the $[x_1, x_2]$ plane.

These two possibilities are refined further into sub-cases depending on the signs of the real part. In the case of real $\lambda^{(1)} > 0$, $\lambda^{(2)} < 0$, x_1 grows exponentially with time, and x_2 contracts exponentially. This behavior, called a saddle, is sketched in figure 4.3, as are the remaining possibilities: in/out nodes, inward/outward spirals, and the center. The magnitude of out-spiral $|x(t)|$ diverges exponentially when $\mu > 0$, and in-spiral contracts into $(0, 0)$ when $\mu < 0$; whereas, the phase velocity ω controls its oscillations.

If eigenvalues $\lambda^{(1)} = \lambda^{(2)} = \lambda$ are degenerate, the matrix might have two linearly independent eigenvectors, or only one eigenvector. We distinguish two cases: (a) A can be brought to diagonal form and (b) A can be brought to Jordan form, which (in

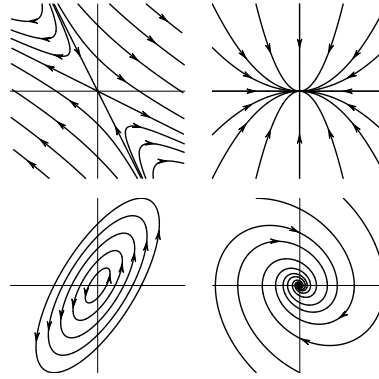
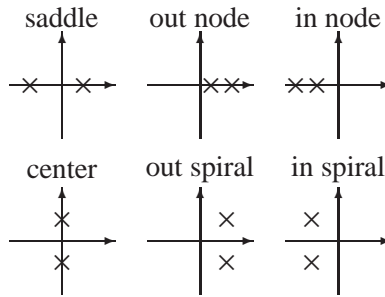


Figure 4.3: Streamlines for several typical 2-dimensional flows: saddle (hyperbolic), in node (attracting), center (elliptic), in spiral.

Figure 4.4: Qualitatively distinct types of exponents $\{\lambda^{(1)}, \lambda^{(2)}\}$ of a $[2 \times 2]$ Jacobian matrix.



dimension 2 or higher) has zeros everywhere except for the repeating eigenvalues on the diagonal and some 1's directly above it. For every such Jordan $[d_a \times d_a]$ block there is only one eigenvector per block.

We sketch the full set of possibilities in figures 4.3 and 4.4, and we work out in detail the most important cases in appendix C, example C.3.

[click to return: p. 81](#)

Example 4.4 In-out spirals. Consider an equilibrium whose stability exponents $\{\lambda^{(1)}, \lambda^{(2)}\} = \{\mu + i\omega, \mu - i\omega\}$ form a complex conjugate pair. The corresponding complex eigenvectors can be replaced by their real and imaginary parts, $\{\mathbf{e}^{(1)}, \mathbf{e}^{(2)}\} \rightarrow \{\text{Re } \mathbf{e}^{(1)}, \text{Im } \mathbf{e}^{(1)}\}$. The 2-dimensional real representation,

$$\begin{pmatrix} \mu & -\omega \\ \omega & \mu \end{pmatrix} = \mu \begin{pmatrix} 1 & 0 \\ 0 & 1 \end{pmatrix} + \omega \begin{pmatrix} 0 & -1 \\ 1 & 0 \end{pmatrix}$$

consists of the identity and the generator of $SO(2)$ rotations in the $\{\text{Re } \mathbf{e}^{(1)}, \text{Im } \mathbf{e}^{(1)}\}$ plane. Trajectories $\mathbf{x}(t) = J^t \mathbf{x}(0)$, where (omitting $\mathbf{e}^{(3)}, \mathbf{e}^{(4)}, \dots$ eigen-directions)

$$J^t = e^{A_q t} = e^{t\mu} \begin{pmatrix} \cos \omega t & -\sin \omega t \\ \sin \omega t & \cos \omega t \end{pmatrix}, \tag{4.33}$$

spiral in/out around $(x, y) = (0, 0)$, see figure 4.3, with the rotation period T . The trajectories contract/expand radially by the multiplier Λ_{radial} and also by the multiplier Λ_j , along the $\mathbf{e}^{(j)}$ eigen-direction per turn of the spiral:

[exercise C.1](#)

$$T = 2\pi/\omega, \quad \Lambda_{\text{radial}} = e^{T\mu}, \quad \Lambda_j = e^{T\mu^{(j)}}. \tag{4.34}$$

We learn that the typical turnover time scale in the neighborhood of the equilibrium $(x, y) = (0, 0)$ is of the order $\approx T$ (and not, let us say, $1000 T$, or $10^{-2} T$). Λ_j multipliers give us estimates of strange-set thickness in eigen-directions transverse to the rotation plane.

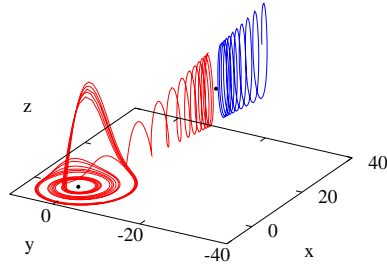


Figure 4.5: Two trajectories of the Rössler flow initiated in the neighborhood of the ‘+’ or ‘outer’ equilibrium point (2.24). (R. Paškauskas)

Example 4.5 Stability of equilibria of the Rössler flow. (continued from example 4.1) The Rössler system (2.23) has two equilibrium points (2.24), the inner equilibrium (x_-, y_-, z_-) , and the outer equilibrium point (x_+, y_+, z_+) . Together with their exponents (eigenvalues of the stability matrix), the two equilibria yield quite detailed information about the flow. Figure 4.5 shows two trajectories which start in the neighborhood of the outer ‘+’ equilibrium. Trajectories to the right of the equilibrium point ‘+’ escape, and those to the left spiral toward the inner equilibrium point ‘-’, where they seem to wander chaotically for all times. The stable manifold of the outer equilibrium point thus serves as the attraction basin boundary. Consider now the numerical values for eigenvalues of the two equilibria:

$$\begin{aligned} (\mu_-^{(1)}, \mu_-^{(2)} \pm i \omega_-^{(2)}) &= (-5.686, \quad 0.0970 \pm i 0.9951) \\ (\mu_+^{(1)}, \mu_+^{(2)} \pm i \omega_+^{(2)}) &= (0.1929, \quad -4.596 \times 10^{-6} \pm i 5.428). \end{aligned} \tag{4.35}$$

Outer equilibrium: The $\mu_+^{(2)} \pm i \omega_+^{(2)}$ complex eigenvalue pair implies that the neighborhood of the outer equilibrium point rotates with angular period $T_+ \approx |2\pi/\omega_+^{(2)}| = 1.1575$. The multiplier by which a trajectory that starts near the ‘+’ equilibrium point contracts in the stable manifold plane is the excruciatingly slow multiplier $\Lambda_2^+ \approx \exp(\mu_+^{(2)} T_+) = 0.9999947$ per rotation. For each period the point of the stable manifold moves away along the unstable eigen-direction by factor $\Lambda_1^+ \approx \exp(\mu_+^{(1)} T_+) = 1.2497$. Hence the slow spiraling on both sides of the ‘+’ equilibrium point.

Inner equilibrium: The $\mu_-^{(2)} \pm i \omega_-^{(2)}$ complex eigenvalue pair tells us that the neighborhood of the ‘-’ equilibrium point rotates with angular period $T_- \approx |2\pi/\omega_-^{(2)}| = 6.313$, slightly faster than the harmonic oscillator estimate in (2.20). The multiplier by which a trajectory that starts near the ‘-’ equilibrium point spirals away per one rotation is $\Lambda_{\text{radial}} \approx \exp(\mu_-^{(2)} T_-) = 1.84$. The $\mu_-^{(1)}$ eigenvalue is essentially the z expansion correcting parameter c introduced in (2.22). For each Poincaré section return, the trajectory is contracted into the stable manifold by the amazing factor of $\Lambda_1 \approx \exp(\mu_-^{(1)} T_-) = 10^{-15.6}$ (!).

Suppose you start with a 1 mm interval pointing in the Λ_1 eigen-direction. After one Poincaré return the interval is of the order of 10^{-4} fermi, the furthest we will get into subnuclear structure in this book. Of course, from the mathematical point of view, the flow is reversible, and the Poincaré return map is invertible. (continued in example 11.3)

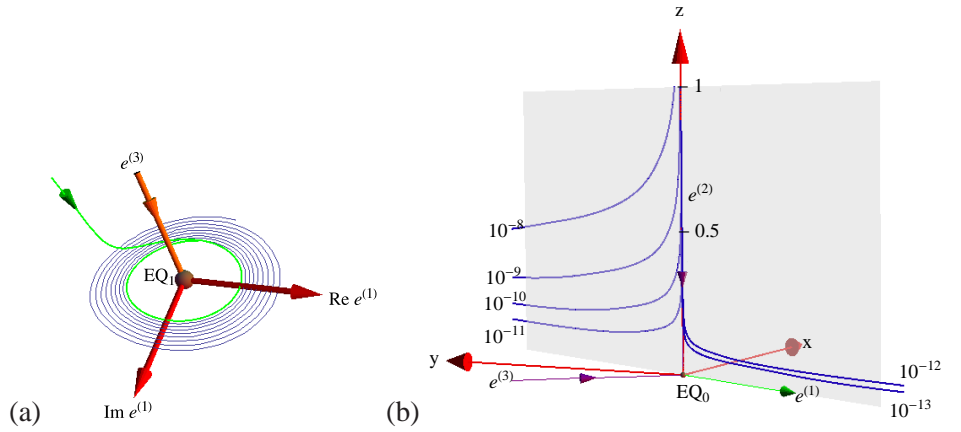
(R. Paškauskas)

Example 4.6 Stability of Lorenz flow equilibria: (continued from example 4.1) A glance at figure 3.4 suggests that the flow is organized by its 3 equilibria, so let us have a closer look at their stable/unstable manifolds.

The E_{Q_0} equilibrium stability matrix (4.30) evaluated at $x_{EQ_0} = (0, 0, 0)$ is block-diagonal. The z -axis is an eigenvector with a contracting eigenvalue $\lambda^{(2)} = -b$. From

remark 9A.13

Figure 4.6: (a) A perspective view of the linearized Lorenz flow near EQ_1 equilibrium, see figure 3.4 (a). The unstable eigenplane of EQ_1 is spanned by $\{\text{Re } \mathbf{e}^{(1)}, \text{Im } \mathbf{e}^{(1)}\}$; the stable subspace by the stable eigenvector $\mathbf{e}^{(3)}$. (b) Lorenz flow near the EQ_0 equilibrium: unstable eigenvector $\mathbf{e}^{(1)}$, stable eigenvectors $\mathbf{e}^{(2)}, \mathbf{e}^{(3)}$. Trajectories initiated at distances $10^{-8} \dots 10^{-12}, 10^{-13}$ away from the z -axis exit finite distance from EQ_0 along the $(\mathbf{e}^{(1)}, \mathbf{e}^{(2)})$ eigenvectors plane. Due to the strong $\lambda^{(1)}$ expansion, the EQ_0 equilibrium is, for all practical purposes, unreachable, and the $EQ_1 \rightarrow EQ_0$ heteroclinic connection never observed in simulations such as figure 2.5. (E. Siminos; continued in figure 11.8.)



(4.41) it follows that all $[x, y]$ areas shrink at the rate $-(\sigma + 1)$. Indeed, the $[x, y]$ submatrix

$$A^- = \begin{pmatrix} -\sigma & \sigma \\ \rho & -1 \end{pmatrix} \quad (4.36)$$

has a real expanding/contracting eigenvalue pair $\lambda^{(1,3)} = -(\sigma + 1)/2 \pm \sqrt{(\sigma - 1)^2/4 + \rho\sigma}$, with the right eigenvectors $\mathbf{e}^{(1)}, \mathbf{e}^{(3)}$ in the $[x, y]$ plane, given by (either) column of the projection operator

$$\mathbf{P}_i = \frac{A^- - \lambda^{(j)} \mathbf{1}}{\lambda^{(i)} - \lambda^{(j)}} = \frac{1}{\lambda^{(i)} - \lambda^{(j)}} \begin{pmatrix} -\sigma - \lambda^{(j)} & \sigma \\ \rho & -1 - \lambda^{(j)} \end{pmatrix}, \quad i \neq j \in \{1, 3\}. \quad (4.37)$$

$EQ_{1,2}$ equilibria have no symmetry, so their eigenvalues are given by the roots of a cubic equation, the secular determinant $\det(A - \lambda \mathbf{1}) = 0$:

$$\lambda^3 + \lambda^2(\sigma + b + 1) + \lambda b(\sigma + \rho) + 2\sigma b(\rho - 1) = 0. \quad (4.38)$$

For $\rho > 24.74$, $EQ_{1,2}$ have one stable real eigenvalue and one unstable complex conjugate pair, leading to a spiral-out instability and the strange attractor depicted in figure 2.5.

All numerical plots of the Lorenz flow are carried out here with the Lorenz parameters set to $\sigma = 10$, $b = 8/3$, $\rho = 28$. We note the corresponding stability exponents for future reference,

$$\begin{aligned} EQ_0 : (\lambda^{(1)}, \lambda^{(2)}, \lambda^{(3)}) &= (11.83, -2.666, -22.83) \\ EQ_1 : (\mu^{(1)} \pm i \omega^{(1)}, \lambda^{(3)}) &= (0.094 \pm i 10.19, -13.85). \end{aligned} \quad (4.39)$$

We also note the rotation period $T_{EQ_1} = 2\pi/\omega^{(1)}$ about EQ_1 and the associated expansion/contraction multipliers $\Lambda^{(i)} = \exp(\mu^{(j)} T_{EQ_1})$ per spiral-out turn:

$$T_{EQ_1} = 0.6163, \quad (\Lambda^{(1)}, \Lambda^{(3)}) = (1.060, 1.957 \times 10^{-4}). \quad (4.40)$$

We learn that the typical turnover time scale in this problem is of the order $T \approx T_{EQ_1} \approx 1$ (and not, let us say, 1000, or 10^{-2}). Combined with the contraction rate (4.41), this tells us that the Lorenz flow strongly contracts state space volumes, by factor of $\approx 10^{-4}$ per mean turnover time.

In the E_{Q_1} neighborhood, the unstable manifold trajectories slowly spiral out, with a very small radial per-turn expansion multiplier $\Lambda^{(1)} \simeq 1.06$ and a very strong contraction multiplier $\Lambda^{(3)} \simeq 10^{-4}$ onto the unstable manifold, figure 4.6(a). This contraction confines, for all practical purposes, the Lorenz attractor to a 2-dimensional surface, which is evident in figure 3.4.

In the $x_{EQ_0} = (0, 0, 0)$ equilibrium neighborhood, the extremely strong $\lambda^{(3)} \simeq -23$ contraction along the $\mathbf{e}^{(3)}$ direction confines the hyperbolic dynamics near E_{Q_0} to the plane spanned by the unstable eigenvector $\mathbf{e}^{(1)}$, with $\lambda^{(1)} \simeq 12$, and the slowest contraction rate eigenvector $\mathbf{e}^{(2)}$ along the z -axis, with $\lambda^{(2)} \simeq -3$. In this plane, the strong expansion along $\mathbf{e}^{(1)}$ overwhelms the slow $\lambda^{(2)} \simeq -3$ contraction down the z -axis, making it extremely unlikely for a random trajectory to approach E_{Q_0} , figure 4.6(b). Thus, linearization describes analytically both the singular dip in the Poincaré sections of figure 3.4 and the empirical scarcity of trajectories close to E_{Q_0} . (continued in example 4.8)

(E. Siminos and J. Halcrow)

Example 4.7 Lorenz flow: Global portrait. (continued from example 4.6) As the E_{Q_1} unstable manifold spirals out, the strip that starts out in the section above E_{Q_1} in figure 3.4 cuts across the z -axis invariant subspace. This strip necessarily contains a heteroclinic orbit that hits the z -axis head on, and in infinite time (but exponentially fast) descends all the way to E_{Q_0} .

How? Since the dynamics is linear (see figure 4.6(a)) in the neighborhood of E_{Q_0} , there is no need to integrate numerically the final segment of the heteroclinic connection. It is sufficient to bring a trajectory a small distance away from E_{Q_0} , continue analytically to a small distance beyond E_{Q_0} and then resume the numerical integration.

What happens next? Trajectories to the left of the z -axis shoot off along the $\mathbf{e}^{(1)}$ direction, and those to the right along $-\mathbf{e}^{(1)}$. Given that $xy > 0$ along the $\mathbf{e}^{(1)}$ direction, the nonlinear term in the z equation (2.18) bends both branches of the E_{Q_0} unstable manifold $W^u(E_{Q_0})$ upwards. Then ... - never mind. We postpone completion of this narrative to example 9A.13, where the discrete symmetry of Lorenz flow will help us streamline the analysis. As we shall show, what we already know about the 3 equilibria and their stable/unstable manifolds suffices to completely pin down the topology of Lorenz flow. (continued in example 9A.13)

(E. Siminos and J. Halcrow)

Example 4.8 Lorenz flow state space contraction: (continued from example 4.6) It follows from (4.30) and (4.29) that Lorenz flow is volume contracting,

$$\partial_i v_i = \sum_{i=1}^3 \lambda^{(i)}(x, t) = -\sigma - b - 1, \tag{4.41}$$

at a constant, coordinate- and ρ -independent rate, set by Lorenz to $\partial_i v_i = -13.66$. For periodic orbits and long time averages, there is no contraction/expansion along the flow, $\lambda^{(ll)} = 0$, and the sum of $\lambda^{(i)}$ is constant by (4.41). Thus, we compute only one independent exponent $\lambda^{(i)}$. (continued in example 9A.13)

[click to return: p. 85](#)

Example 4.9 Stability of a 1-dimensional map: Consider the orbit $\{\dots, x_{-1}, x_0, x_1, x_2, \dots\}$ of a 1-dimensional map $x_{n+1} = f(x_n)$. When studying linear stability (and higher derivatives) of the map, it is often convenient to use a local coordinate system z_a centered on the orbit point x_a , together with a notation for the map, its derivative, and, by the chain rule, the derivative of the k th iterate f^k evaluated at the point x_a ,

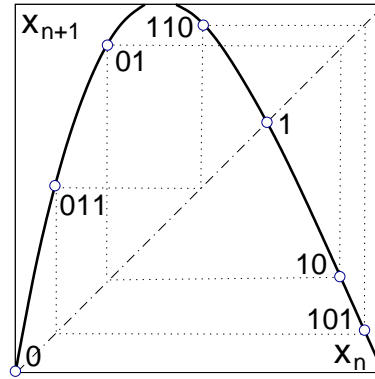


Figure 4.7: A unimodal map, together with fixed points 0, 1, 2-cycle 01 and 3-cycle 011.

$$\begin{aligned}
 x &= x_a + z_a, & f_a(z_a) &= f(x_a + z_a) \\
 f'_a &= f'(x_a) \\
 \Lambda(x_0, k) &= f'_a{}^k = f'_{a+k-1} \cdots f'_{a+1} f'_a, & k &\geq 2.
 \end{aligned}
 \tag{4.42}$$

Here a is the label of point x_a , and the label $a+1$ is shorthand for the next point b on the orbit of x_a , $x_b = x_{a+1} = f(x_a)$. For example, a period-3 periodic point in figure 4.7 might have label $a = 011$, and by $x_{110} = f(x_{011})$ the next point label is $b = 110$.

[click to return: p. 82](#)

Example 4.10 Hénon map Jacobian matrix: For the Hénon map (3.17) the Jacobian matrix for the n th iterate of the map is

$$M^n(x_0) = \prod_{m=n}^1 \begin{pmatrix} -2ax_m & b \\ 1 & 0 \end{pmatrix}, \quad x_m = f_1^m(x_0, y_0).
 \tag{4.43}$$

The determinant of the Hénon one time-step Jacobian matrix (4.43) is constant,

$$\det M = \Lambda_1 \Lambda_2 = -b.
 \tag{4.44}$$

In this case only one eigenvalue $\Lambda_1 = -b/\Lambda_2$ needs to be determined. This is not an accident; a constant Jacobian was one of desiderata that led Hénon to construct a map of this particular form.

[click to return: p. 83](#)

Exercises

4.1. **Trace-log of a matrix.** Prove that

$$\det M = e^{\text{tr} \ln M}.$$

for an arbitrary nonsingular finite dimensional matrix M , $\det M \neq 0$.

4.2. **Stability, diagonal case.** Verify the relation (4.32)

$$J^t = e^{tA} = \mathbf{U}^{-1} e^{tA_D} \mathbf{U}, \quad A_D = \mathbf{U} \mathbf{A} \mathbf{U}^{-1}.$$

4.3. **State space volume contraction.**

- (a) Compute the Rössler flow volume contraction rate at the equilibria.
- (b) Study numerically the instantaneous $\partial_i v_i$ along a typical trajectory on the Rössler attractor; color-code the points on the trajectory by the sign (and perhaps the magnitude) of $\partial_i v_i$. If you see regions of local expansion, explain them.
- (c) (optional) Color-code the points on the trajectory by the sign (and perhaps the magnitude) of

$$\partial_i v_i - \overline{\partial_i v_i}.$$

(R. Paškauskas)

- (d) Compute numerically the average contraction rate (4.29) along a typical trajectory on the Rössler attractor. Plot it as a function of time.
- (e) Argue on basis of your results that this attractor is of dimension smaller than the state space $d = 3$.
- (f) (optional) Start some trajectories on the escape side of the outer equilibrium, and color-code the points on the trajectory. Is the flow volume contracting?

(continued in exercise 20.10)

4.4. **Topology of the Rössler flow.** (continuation of exercise 3.1)

- (a) Show that equation $|\det(A - \lambda \mathbf{1})| = 0$ for Rössler flow in the notation of exercise 2.8 can be written as

$$\lambda^3 + \lambda^2 c (p^\mp - \epsilon) + \lambda (p^\pm / \epsilon + 1 - c^2 \epsilon p^\mp) \mp c \sqrt{D} = 0 \quad (4.45)$$

- (b) Solve (4.45) for eigenvalues λ^\pm for each equilibrium as an expansion in powers of ϵ . Derive

$$\begin{aligned} \lambda_1^- &= -c + \epsilon c / (c^2 + 1) + o(\epsilon) \\ \lambda_2^- &= \epsilon c^3 / [2(c^2 + 1)] + o(\epsilon^2) \\ \theta_2^- &= 1 + \epsilon / [2(c^2 + 1)] + o(\epsilon) \\ \lambda_1^+ &= c\epsilon(1 - \epsilon) + o(\epsilon^3) \\ \lambda_2^+ &= -\epsilon^5 c^2 / 2 + o(\epsilon^6) \\ \theta_2^+ &= \sqrt{1 + 1/\epsilon} (1 + o(\epsilon)) \end{aligned} \quad (4.46)$$

Compare with exact eigenvalues. What are dynamical implications of the extravagant value of λ_1^- ? (continued as exercise 13.7)

4.5. **Time-ordered exponentials.** Given a time dependent matrix $A(t)$ check that the time-ordered exponential

$$J(t) = \mathbf{T} e^{\int_0^t d\tau A(\tau)}$$

may be written as

$$J(t) = \sum_{m=0}^{\infty} \int_0^t dt_1 \int_0^{t_1} dt_2 \cdots \int_0^{t_{m-1}} dt_m A(t_1) \cdots A(t_m)$$

and verify, by using this representation, that $J(t)$ satisfies the equation

$$\dot{J}(t) = A(t)J(t),$$

with the initial condition $J(0) = 1$.

4.6. **A contracting baker's map.** Consider a contracting (or 'dissipative') baker's map, acting on a unit square $[0, 1]^2 = [0, 1] \times [0, 1]$, defined by

$$\begin{aligned} \begin{pmatrix} x_{n+1} \\ y_{n+1} \end{pmatrix} &= \begin{pmatrix} x_n/3 \\ 2y_n \end{pmatrix} & y_n \leq 1/2 \\ \begin{pmatrix} x_{n+1} \\ y_{n+1} \end{pmatrix} &= \begin{pmatrix} x_n/3 + 1/2 \\ 2y_n - 1 \end{pmatrix} & y_n > 1/2. \end{aligned}$$

This map shrinks strips by a factor of 1/3 in the x -direction, and then it stretches (and folds) them by a factor of 2 in the y -direction.

By how much does the state space volume contract for one iteration of the map?

References

[4.1] C. D. Meyer, *Matrix Analysis and Applied Linear Algebra*, (SIAM, Philadelphia 2001).

[4.2] G. H. Golub and C. F. Van Loan, *Matrix Computations* (J. Hopkins Univ. Press, Baltimore, MD, 1996).

[4.3] T. F. Coleman and C. Van Loan, *Handbook for Matrix Computations* (SIAM, Philadelphia, 1988).

[4.4] D. S. Watkins, *The Matrix Eigenvalue Problem: GR and Krylov Subspace Methods* (SIAM, Philadelphia, 2007).

[4.5] D. S. Watkins, *Fundamentals of Matrix Computations* (Wiley, New York, 2010).

[4.6] M. W. Hirsch and S. Smale, *Differential Equations, Dynamical Systems, and Linear Algebra*, (Academic Press, San Diego 1974).

- [4.7] V.I. Arnold, *Ordinary Differential Equations*, (Mit Press, Cambridge 1978).
- [4.8] E. M. Izhikevich, “Equilibrium,” www.scholarpedia.org/article/Equilibrium.
- [4.9] P. Holmes and E. T. Shea-Brown, “Stability,” www.scholarpedia.org/article/Stability.
- [4.10] J. D. Meiss, *Differential Dynamical Systems* (SIAM, Philadelphia 2007).
- [4.11] L. Perko, *Differential Equations and Dynamical Systems* (Springer-Verlag, New York 1991).
- [4.12] P. Glendinning, *Stability, Instability, and Chaos* (Cambridge Univ. Press, Cambridge 1994).
- [4.13] L. N. Trefethen and D. Bau, *Numerical Linear Algebra* (SIAM, Philadelphia 1997).
- [4.14] E. N. Lorenz, A study of the predictability of a 28-variable atmospheric model, *Tellus* **17**, 321 (1965).
- [4.15] M. Tabor, Sect 1.4 “Linear stability analysis,” in *Chaos and Integrability in Nonlinear Dynamics: An Introduction* (Wiley, New York 1989), pp. 20-31.
- [4.16] C. Skokos, “Alignment indices: a new, simple method for determining the ordered or chaotic nature of orbits,” *J. Phys A* **34**, 10029 (2001).
- [4.17] C. Skokos, “The Lyapunov Characteristic Exponents and their computation,” [arXiv:0811.0882](https://arxiv.org/abs/0811.0882).
- [4.18] I. Goldhirsch, P. L. Sulem, and S. A. Orszag, Stability and Lyapunov stability of dynamical systems: A differential approach and a numerical method, *Physica D* **27**, 311 (1987).
- [4.19] T. Manos, C. Skokos, and C. Antonopoulos, Probing the local dynamics of periodic orbits by the generalized alignment index (GALI) method, [arXiv:1103.0700](https://arxiv.org/abs/1103.0700), 2011.
- [4.20] C. G. J. Jacobi, “De functionibus alternantibus earumque divisione per productum e differentiis elementorum conflatum,” in *Collected Works*, Vol. 22, 439; *J. Reine Angew. Math. (Crelle)* (1841).
- [4.21] wikipedia.org, “*Routh-Hurwitz stability criterion*.”
- [4.22] G. Meinsma, “Elementary proof of the *Routh-Hurwitz test*,” *Systems and Control Letters* **25** 237 (1995).
- [4.23] K. Ramasubramanian and M.S. Sriram, “A comparative study of computation of Lyapunov spectra with different algorithms,” *Physica D* **139**, 72 (2000).
- [4.24] J.-L. Thiffeault, Derivatives and constraints in chaotic flows: asymptotic behaviour and a numerical method, *Physica D* **172**, 139 (2002), [arXiv:nlin/0101012](https://arxiv.org/abs/nlin/0101012).

- [4.25] J. M. Ottino, *The Kinematics of Mixing: Stretching, Chaos and Transport* (Cambridge Univ. Press, Cambridge, 1989).
- [4.26] R. A. Horn and C. R. Johnson, *Matrix Analysis* (Cambridge Univ. Press, Cambridge, 1990).